Design and Implementation of Polyester-Based Textile Antenna for Smart Clothing

Md. Samiul Islam and Abu Zafor Md. Touhidul Islam

***Abstract*—In the present study, a newly designed polyester substrate-based textile microstrip patch antenna operating in the 3.5 GHz band is proposed for smart clothing in broadband wireless applications. The motivation behind this work stems from the lack of comprehensive studies that address all critical aspects—including off-body performance, fabrication, testing, on-body evaluation, bending analysis, and SAR assessment—while specifically focusing on polyester textile antenna designs for the 3.5 GHz band in next-generation wearable systems. The antenna of small dimension 30×20×0.8 mm³ is designed and simulated in CST, followed by prototype fabrication and subsequent measurements to validate the simulation results. Slotting and partial grounding techniques are employed in the design for improving the radiation performance of the antenna. The effectiveness of the antenna has been assessed under the off-body and on-body conditions. Bending analysis under various bending conditions is performed to assess the antenna's flexibility and suitability for wearable applications. Experimental results obtained from the fabricated antenna in free space and on-body scenarios show agreement with simulation data. Moreover, the specific absorption rate (SAR) analysis confirming that the antenna complies with IEEE safety standards. The proposed antenna achieves a wide bandwidth of 1.17 GHz (operating range of 3.11-4.27 GHz), a higher radiation efficiency of 94.52%, and a moderate peak gain of 2.59 dB. It covers 5G NR (n77, n78), C-Band (Radar/WiMAX), CBRS, and Extended C-Bands used for wearable broadband applications. Hence, the proposed antenna is robust and well-suited for smart clothing applications in wireless broadband applications as it combines good radiation characteristics and stable performance under bending, while maintaining safe SAR levels and a compact textile-compatible design.**

***Index Terms*—Polyester substrate, smart clothing, textile antenna, wearable, wireless broadband.**

Original Research Paper
DOI: 10.53314/ELS2630039I

Manuscript received on November 7th, 2025. Received in revised form on March 15th and April 16th, 2026. Accepted for publication on April 27th, 2026.

Md. Samiul Islam is with the Antenna Design Lab, Department of Electrical and Electronic Engineering, University of Rajshahi, Rajshahi 6205, Bangladesh (e-mail: samiulislam.ru64@gmail.com, ORCiD: 0009-0004-8345-3204).

Abu Zafor Md. Touhidul Islam is with the Antenna Design Lab, Department of Electrical and Electronic Engineering, University of Rajshahi, Rajshahi 6205, Bangladesh (e-mail: touhid.eee@ru.ac.bd, ORCiD 0009-0002-0375-4660).

I. Introduction

A rapid increase in research on body-centric wireless communication and wearable devices has been observed in recent years, attributed to their diverse applications in personal communication systems. Wearable electronics are utilized across various fields, including sports, defense, space missions, mobile medical monitoring, and general healthcare. [1]-[3]. Smart clothing refers to clothing enhanced with technology to sense and react to the wearer's body or environment. It integrates electronic components like sensors, conductive fabrics, and microcontrollers, permitting it to monitor biometrics, adjust to conditions, and even communicate with other devices. Smart textile antennas are increasingly preferred for their low cost, high flexibility, simple manufacturing procedures, lightweight, and comfort for wearable on-body applications [4]. Various antenna types including microstrip, dipole, monopole, loop, slot, and planar inverted-F (PIFA) designs are well-suited for smart textile integration. Textile antennas typically utilize materials such as polyester, cotton, denim, and plastics as dielectric substrates, combined with conductive radiating layers, to achieve the flexibility and wearability needed for garment integration [5], [6].

However, key challenges in designing textile antennas for smart clothing include maintaining antenna performance and reliability while ensuring flexibility, comfort and washability. To mitigate these challenges, researchers are exploring various approaches such as optimizing material selection and antenna geometry for various body movements, utilizing advanced fabrication techniques, addressing specific absorption rate (SAR) concerns, and so on [7]. A denim-based textile antenna introduced in [8] supports tri-band operation resonates at 2.13, 4.75, and 11.495 GHz, making it suitable for wireless systems used in emergency and surveillance contexts. A textile antenna with breathable and flexible properties was introduced in [9], operating at 2.45 GHz and incorporating a 3D spacer substrate to facilitate airflow. To enhance bandwidth, an E-shaped slot design was proposed in [10]. Despite these advancements, developing a wideband textile antenna that maintains durability and reliable data transmission under varying human body postures remains a critical challenge. Authors in [11] suggested Multiple-input multiple-output antenna as a viable approach to overcoming such limitations. In [12], a textile antenna tailored for integration into smart garments was designed, fabricated, and experimentally validated to match the simulated performance at 2.45 GHz. Bending and on-body performance analysis have also been performed.

Zhou et al. [13] introduced a circular-shaped textile antenna for wireless body area network (WBAN) services featuring dual-band (2.45 GHz and 5.8 GHz) and dual-polarization characteristics. Its performance is assessed under off-body, on-body and bending conditions. A frequency-reconfigurable textile antenna was designed and fabricated in [14] for wearable applications. In the design, denim was used as substrate, while a single PIN diode was employed to shift between the bands. Kivata et al. in [15] proposed a compact wearable textile antenna of size 30 × 30 mm². The antenna was designed to resonate at 3.4 GHz, and employs denim, jeans, and FR-4 substrate materials for applications in wireless broadband.

Although the stated antennas showed promising results for wearable applications, in most cases, they had larger sizes, narrow bandwidths, expensive substrates, and so on. Therefore, continuous advances in research are now focused on wideband, low-cost, and miniaturized antennas for wearable applications. Moreover, there's a noticeable gap in studies focusing on textile antenna designs specifically for the 3.5 GHz band, particularly for broadband wireless communication. Existing research primarily concentrates on other 5G frequencies like (2.4 - 2.484 GHz), WiMAX (2-11 GHz), and other WLAN bands. The 3.5 GHz band is relevant for various applications including telemedicine, m-health (mobile health), and e-health, making it a crucial area for further investigation. While very few studies exist on textile antenna design at 3.5 GHz [15]-[18], a comprehensive study covering all aspects such as off-body analysis, fabrication, testing, on-body analysis, bending analysis, and SAR analysis is currently lacking.

This study presents a novel polyester-based small textile patch antenna at 3.5 GHz suitable for smart clothing in wireless broadband applications. Polyester was selected as the substrate material for the antenna due to its advantageous combination of properties, including a low dielectric constant, high mechanical flexibility, lightweight and thin profile, resistance to moisture, cost-effectiveness, and widespread availability. The low dielectric constant helps to reduce surface wave losses and contributes to broader bandwidth and better radiation efficiency, especially in microstrip patch antennas. Polyester is soft, bendable, and resilient, making it ideal for integration into clothing without compromising comfort or durability. It is lightweight, inexpensive and can be manufactured in thin layers, making it a practical choice for low-profile wearable antenna designs. Compared to natural fibers like cotton, polyester absorbs less moisture, which helps to maintain stable electromagnetic properties even in humid environments. Furthermore, polyester demonstrates superior durability against washing, mechanical deformation, and environmental exposure, making it suitable for long-term wearable antenna applications.

This research is focused on designing a compact polyester-based antenna at 3.5 GHz and improving its efficiency, bandwidth, and reliability to make them viable alternatives to conventional substrates, and to make them promising for wearable and smart clothing applications. The optimized antenna dimensions are 30×20×0.8 mm³, which is notably small compared to many textile antennas, making it more practical for integration into wearable devices. The antenna resonates at 3.5 GHz and achieves a wide operating range of 3.11–4.27 GHz, covering several key communication bands 3.3–3.8 GHz (5G NR (n77, n78) band), 3.1–3.7 GHz (C-Band Radar / WiMAX band), 3.5 GHz (Citizens Broadband Radio Service (CBRS) band), and 4.0–4.2 GHz (Extended C-Band) that are highly relevant for modern wearable applications in smart clothing, sports, and healthcare. Novel implementation of slotting and partial grounding helps to improve bandwidth and efficiency. In addition, the bending analysis is performed, and the antenna's performance is tested under off-body and on-body conditions, ensuring reliability in real-world wearable scenarios. The simulation and numerical performance analysis were carried out using CST Studio software. The antenna prototype was fabricated, and the performance parameters (return loss and VSWR) were measured to validate the simulation results.

The rest of the paper is arranged as follows. The antenna design approach is discussed in Section II. Antenna Fabrication and Testing procedures are presented in Section III. Section IV presents the results and discussion, including simulation and experimental results under off-body and on-body conditions, as well as bending and SAR analyses. A comparison of the proposed antenna's performance with previously reported designs is given in Section V. Finally, key findings of the research are listed in Section VI.

II. Antenna Design Approach

Initially, the proposed antenna's design, simulation, parametric investigation, and numerical analysis were carried out in CST under the off-body (free space) condition. The prototype is then fabricated and the performance metrics are measured in the laboratory using the vector network analyzer (VNA). After that numerical analysis under the on-body condition, bending analysis and SAR analysis were performed in CST.

Fig. 1 describes the construction of the projected antenna designed to resonate at 3.5GHz. A 0.8 mm thick polyester textile material with a dielectric constant and a loss tangent of 1.9 and 0.0045, respectively, was used as the substrate. The patch, feed line, and ground plane were made from conductive copper tape with a thickness of 0.035 mm. The design employs a microstrip feed line to deliver power to the radiating patch element of the antenna. Initially, using the following set of basic equations, the antenna size was estimated for 3.5 GHz resonance frequency. After that, the antenna design was optimized to a net size of 30 × 20 × 0.8 mm³. A set of rectangular slots on the patch plane and a partial grounding structure were added to improve impedance matching and effectiveness of the antenna.

Width of the patch is $$W_p = \frac{c_0}{2f_r\sqrt{\frac{2}{\epsilon_r+1}}} \qquad (1)$$

where c_0= light speed in free space, f_r= resonance frequency, ϵ_r= substrate dielectric constant.

Length is $$L = 0.412h\frac{(\epsilon_{reff}+0.3)\,(\frac{W_p}{h}+0.264)}{(\epsilon_{reff}-0.258)\,(\frac{W_p}{h}+0.8)} \qquad (2)$$

where $$\epsilon_{reff} = \frac{\epsilon_r+1}{2} + \frac{\epsilon_r-1}{2}\left[1+12\frac{h}{W}\right]^{-\frac{1}{2}} \quad (3)$$

ϵ_{reff} is effective dielectric constant, h is substrate thickness.

Effective length is $$L_{eff} = \frac{c_0}{2f_r\sqrt{\epsilon_{reff}}} \quad (4)$$

Patch length is $$L_p = L_{eff} - 2\Delta L \quad (5)$$

The optimized parameters of the projected antenna are shown in Table I. The patch is placed on the top surface of the textile substrate. The optimized size of the substrate and patch are 30 mm × 20 mm and 12.65 mm × 14.64 mm, respectively. The antenna comprises a right-angle triangular slot (p = q = 3 mm, r = 4.24 mm) and rectangular slots (Li1= =12.75 mm, Li2=8.75 mm, W1= 2 mm). A microstrip feedline with dimension of 15 mm × 2.58 mm was used to excite the patch. Fig. 1(a) shows the designed antenna's front view while Fig. 1(b) illustrates the rear view.

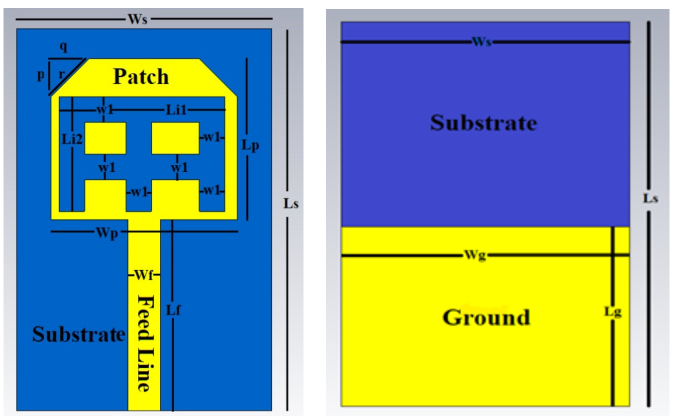

(a) (b)

Fig. 1. (a) front view, (b) rear view of the proposed antenna.

TABLE I
Optimized of Design Parameters of the Proposed Antenna

Parameters	Values (mm)
Substrate Width, Ws	20
Substrate Length, Ls	30
Feed Line Length, Lf	15
Feed Line Width, Wf	2.58
Patch Length, Lp	12.65
Patch Width, Wp	14.64
Ground Width, Wg	20
Ground Length, Lg	14
Substrate Height, h	0.8
Li1	12.5
Li2	8.75
W1	2.0
p	3.0
q	3.0
r	4.24

Incorporation of slotting and partial grounding plays a significant role in performance improvement of the antenna. Slotting enhances antenna performance by reshaping current distribution, introducing multiple resonances, improving impedance matching, and boosting radiation efficiency. These mechanisms collectively contribute to wider bandwidth, better efficiency, and more compact designs. On the other hand, partial grounding in antenna design improves performance by optimizing impedance matching, broadening bandwidth, enhancing radiation efficiency, and enabling more compact and versatile structures. It modifies the electromagnetic interaction between the radiator and the ground plane, leading to better control of current distribution and radiation characteristics.

III. Antenna Fabrication and Testing

Simulations rely on idealized or estimated values (e.g., dielectric constant, loss tangent) are powerful for initial design, but fabricating and measuring a physical antenna prototype prototypes is essential for validating real-world performance. The proposed antenna was fabricated in the laboratory, and its reflection coefficient (S11) and voltage standing wave ratio (VSWR) are measured under the off-body condition in free space and on different parts of the human body using the vector network analyzer (model: LiteVNA 64). Due to the measuring limitations of the VNA and the absence of an anechoic chamber in the laboratory, the gain, efficiency and radiation pattern of the antenna were not measured. The structure of the fabricated antenna is presented in Fig. 2, whereas Fig. 3 depicts the experimental setup.

(a) (b)

Fig. 2. (a) Front and (b) back view of the fabricated antenna.

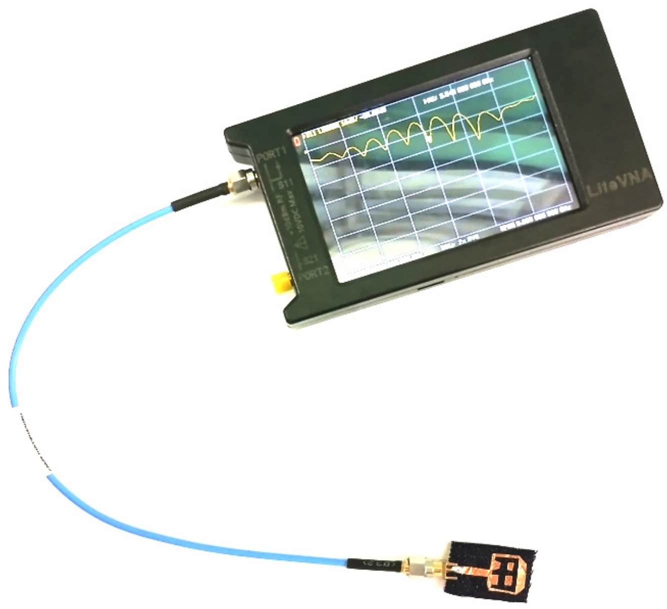

Fig. 3. Setup for measurement.

IV. Results and discussion

A. Off-body Performance Results

1) Reflection Coefficient (S11) and VSWR

A comparison between the simulated and measured reflection coefficient (S11 parameter) and voltage standing wave ration (VSWR) of the proposed antenna is depicted in Fig. 4. The simulation results show that the antenna resonates at ~3.50 GHz. The numerical and experimental resonant peak frequencies of 3.5 GHz and 3.54 GHz are close to each other. The measured resonance peak frequency is ~3.52 GHz, slightly shifted the right from 3.50 GHz. The difference between the two is ~20 MHz, which is less than 1% of the center frequency indicating a very close match and there is strong agreement between the simulation and experimental results. The numerical and measured S11 values are -60.73 dB and -45.42 dB, respectively, indicating the proposed antenna is well matched to the system. Bandwidth is typically defined as the frequency range over which the reflection coefficient (S_{11}) is below −10 dB, meaning less than 10% of the power is reflected. The simulated bandwidth is 1.17 GHz centered around 3.5 GHz, roughly spanning from 3.11 GHz to 4.27 GHz, which covers several key communication bands such as 3.3–3.8 GHz (5G NR (n77, n78) band), 3.1–3.7 GHz (C-Band Radar / WiMAX band), 3.5 GHz (Citizens Broadband Radio Service (CBRS) band), and 4.0–4.2 GHz (Extended C-Band), which are highly relevant for modern wearable broadband applications in smart clothing, sports, and healthcare. The measured bandwidth is slightly broader, extending approximately from 3.35 GHz to 3.65 GHz.

Simulated VSWR minimum value of 0.98 occurred around 3.51 GHz, while measured VSWR minimum value of 1.16 obtained around 3.53 GHz, indicating good impedance matching and the antenna system is highly efficient with minimal signal loss. The close match between simulated and measured VSWR minima and resonance points suggesting accurate simulation modeling, good fabrication and measurement practices, and reliable performance of the device at its intended operating frequency.

Deviations between simulation and measurement results may arise from practical limitations in fabrication, inherent variability in material properties, and differences between idealized simulation boundaries and real-world measurement environments. Minor deviations in slot size, substrate thickness, feed alignment, or soldering can shift resonance, alter impedance, and introduce parasitic effects. Imperfect edges or roughness can interrupt current flow, leading to performance variations. Simulations adopt ideal materials values, but real substrates vary with manufacturing, humidity, and temperature. Small shifts in dielectric constant affect resonance, gain and bandwidth. Simulations assume ideal free-space and matched boundaries, while real tests are affected by fittings, cables, and connectors. Finite ground planes and nearby objects may alter radiation and impedance. Reflections from lab walls, instruments, or people can further distort results compared to simulations.

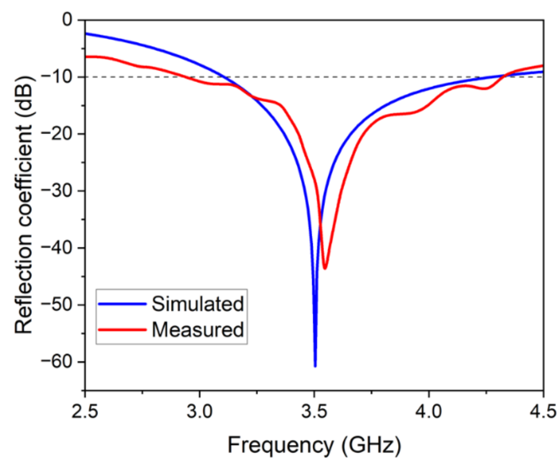

(a)

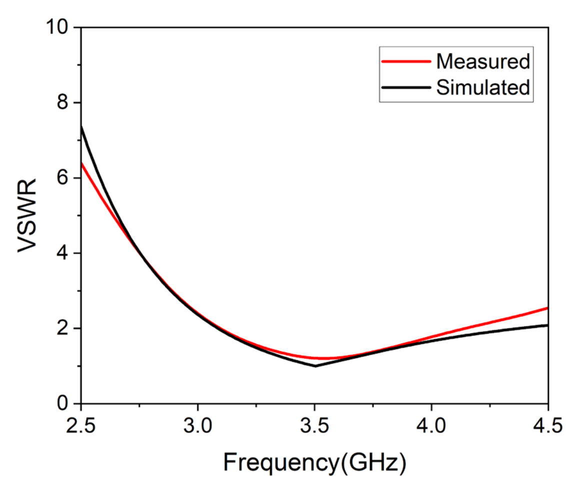

(b)

Fig. 4. Simulated and measured (a) S11, (b) VSWR.

2) Gain and Directivity

The three-dimensional (3D) far-field gain and directivity patterns of the proposed antenna at the resonant frequency of 3.5 GHz are depicted in Fig. 5. The color scale represents the magnitude of radiation intensity or gains in different directions. Red/Orange regions represent high radiation intensity or high gain in that direction (main lobes). Blue regions present low radiation intensity or lower gain (nulls or side lobes). The gradient visually maps how energy is distributed spatially around the antenna.

The proposed antenna exhibits a peak gain of 2.59 dBi and a peak directivity of 2.84 dBi. Directivity represents the ideal radiation pattern assuming no losses. Gain reflects the actual radiated power, incorporating losses from dielectric, conductor, and impedance mismatch. The small difference between the peak values (2.84 vs. 2.59 dBi) indicates high radiation efficiency, approximately 91.2%. The small gap between gain and directivity across figures confirms minimal resistive and dielectric losses.

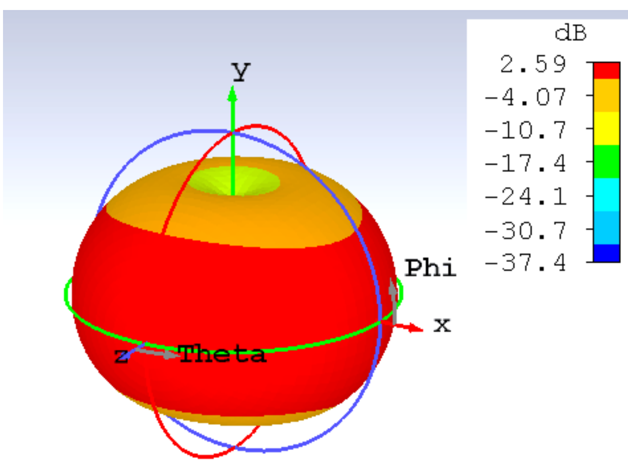

(a)

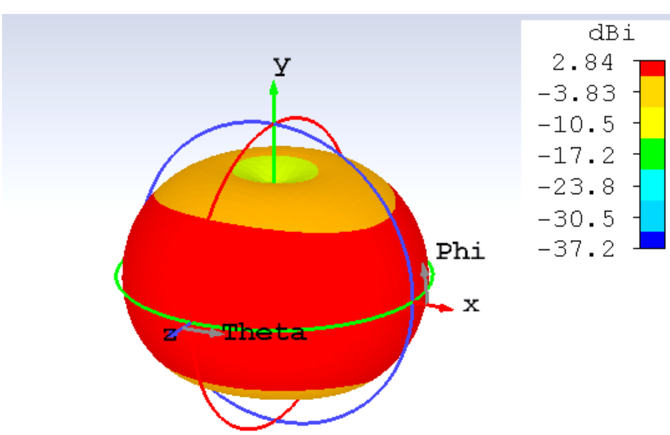

(b)

Fig. 5. 3D farfield gain (a) and directivity (b) at 3.5 GHz.

A 2.59 dBi antenna gain can be adequate for short-range communication or when the antenna is placed in close proximity to the body for on-body communication applications, but its suitability depends on the specific requirements of the system and the environment in which it operates. A directivity of 2.84 dBi can be sufficient for wearable communication applications. It can provide adequate signal strength for short-range, on-body communication.

3) Efficiency

Fig. 6 illustrates the frequency-dependent variation of the radiation efficiency and total efficiency of the designed antenna. At 3.5 GHz, the antenna exhibits a radiation efficiency is 94.54% and total efficiency of 94.52%. The antenna exhibits stable radiation efficiency in the range of 84.52% to 95.84% over the operating frequency range. Accordingly, the proposed antenna demonstrates satisfactory efficiency at its resonant frequency. A radiation efficiency of 94.54% is generally considered very good and more than sufficient for wearable communication applications. A high radiation efficiency means that a large portion of the power fed into the antenna is radiated outwards as an electromagnetic wave, minimizing losses within the antenna itself.

Fig. 5 provides a snapshot of how the antenna radiates energy at 3.5 GHz, showing strong lobes and minimal nulls indicating good directivity and gain. Fig. 6 confirms that this performance is not isolated: the antenna maintains high radiation efficiency across a broad frequency range, peaking near 3.3 GHz, which aligns well with the 3.5 GHz performance in Fig. 5. The efficiency gap between radiation and total efficiency in Fig. 6 mirrors the gain–directivity gap in Fig. 5, reinforcing the interpretation of ~91% efficiency. The antenna is well-optimized around 3.3–3.5 GHz, with high radiation efficiency and strong directional performance.

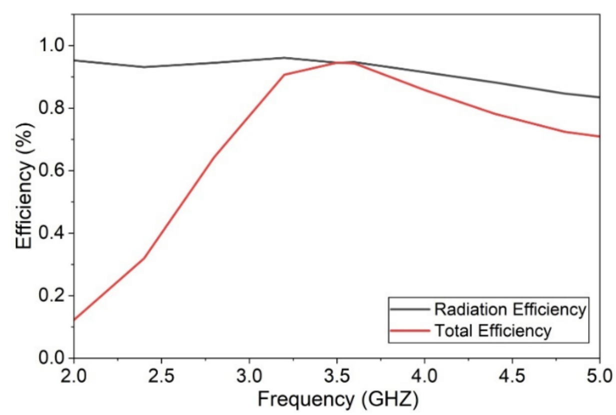

Fig. 6. Efficiency of the proposed antenna.

4) Radiation Pattern

Body-centric environments involve dynamic movements and orientations. Evaluation of E-field patterns at different φ (phi) planes is essential for assessing the angular stability and robustness of wearable antennas. Different φ planes interact differently with the human body's geometry and dielectric properties. Stable E-field patterns across φ planes imply the antenna can maintain performance under body movement, bending, or rotation. Fig. 7 illustrates the simulated electric field (E-field) pattern of the proposed antenna.

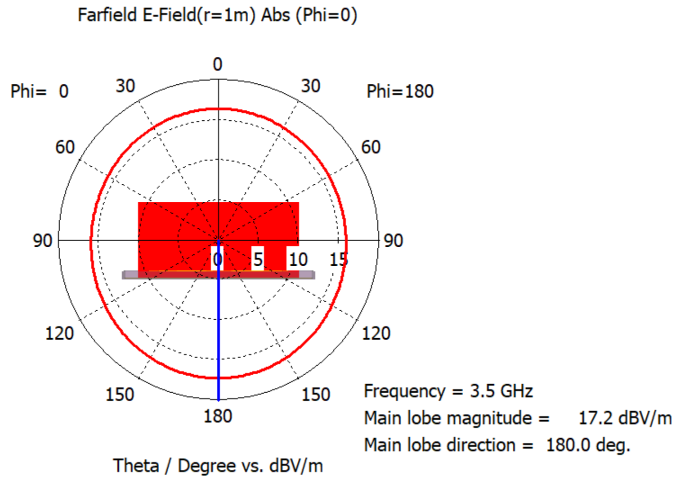

(a)

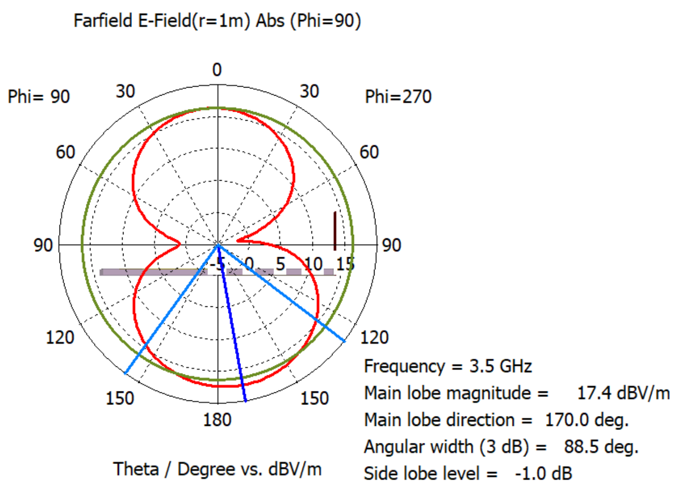

(b)

Fig. 7. Farfield E-field pattern at 3.5 GHz for (a) phi=0, (b) phi=90 degrees.

At the resonant frequency of 3.5 GHz and for φ = 0°, the main lobe magnitude is 17.2 dB V/m, with the main lobe directed at 180°. For φ = 90°, the main lobe magnitude increases slightly to 17.4 dB V/m, maintaining the same direction of 180°. The 3 dB angular beamwidth, and the side-lobe level are 88.5° and -1.0 dB, respectively.

Fig. 5 illustrates the 3D far-field radiation characteristics of the proposed antenna at 3.5 GHz, where the gain and directivity plots exhibit a predominantly spherical radiation envelope, indicating that the antenna radiates energy in multiple directions with relatively uniform intensity. The color-coded surface, mapped in spherical coordinates (Phi, Theta), reveals a quasi-omnidirectional pattern, where the radiated power is distributed broadly across the azimuthal plane with moderate variation in elevation. This pattern is particularly evident in the gain plot, where the absence of sharp nulls and the smooth gradient suggest consistent radiation coverage, making the antenna suitable for applications requiring broad spatial coverage for wireless broadband applications.

5) Surface Current Distribution

Fig. 8 shows the surface current distribution of the proposed textile antenna at 3.5 GHz. The results show that the antenna maintains a clear resonance dip around 3.5 GHz across all bending angles, and S11 lies below –10 dB within the intended operating band, which indicating good impedance matching and stable performance under severe deformation. As the antenna bending angle increases, the resonance peak shifts toward lower frequencies in most cases. These results are consistent with previous studies on bending conditions [19], [20]. The left shift of resonance under bending conditions occurs because with increasing bending angles the antenna's effective electrical length and dielectric loading increase, and lowering the resonant frequency. The antenna's wide bandwidth (1.17 GHz) offers the advantage of even with bending-induced detuning, the antenna covers the target frequency range without performance loss.

Current originates from the microstrip feed line feed and is predominantly distributed across the antenna structure, indicating that the entire antenna actively contributes to resonance at this frequency. The peak surface current density, measured at 85.29 A/m, predominantly accumulates around the lower segment of the feed line and the bottom edges of the patch, as depicted in Fig. 8.

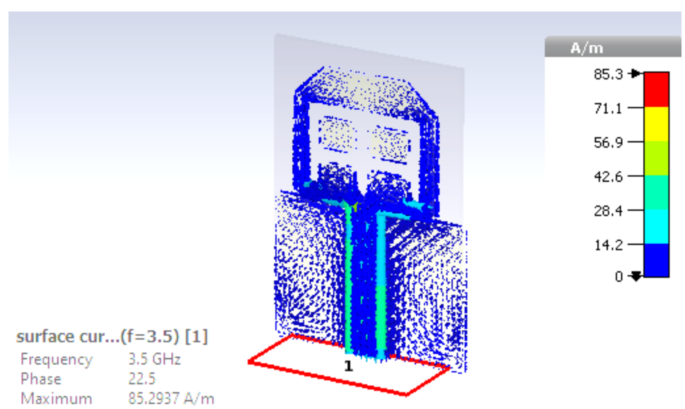

Fig. 8 Surface current distribution at 3.5 GHz.

B. Bending Analysis

Wearable antennas incorporated into garments are not limited to flat configurations; they also undergo mechanical deformations such as bending, stretching, and flexing during regular use [18]. Ten distinct bending situations (from 0° (flat) to 170° (extreme bend)) are chosen for the performance analysis of the proposed antenna. Fig. 9 shows the bended antenna images at four typical bending angles (0°, 30°, 60°, 90°), whereas Fig. 10 presents the S11 versus frequency graphs for all bending angles. As seen, the antenna maintains a clear resonance dip around 3.5 GHz across all bending angles, and S11 lies below –10 dB within the intended operating band, which indicating good impedance matching and stable performance under severe deformation. As the antenna bending angle increases, the resonance peak shifts toward lower frequencies in most cases. These results are consistent with previous studies on bending conditions [19], [20]. The left shift of resonance under bending conditions occurs because with increasing bending angles the antenna's effective electrical length and dielectric loading increase, and lowering the resonant frequency. The antenna's wide bandwidth (1.17 GHz) offers the advantage of even with bending-induced detuning, the antenna covers the target frequency range without performance loss.

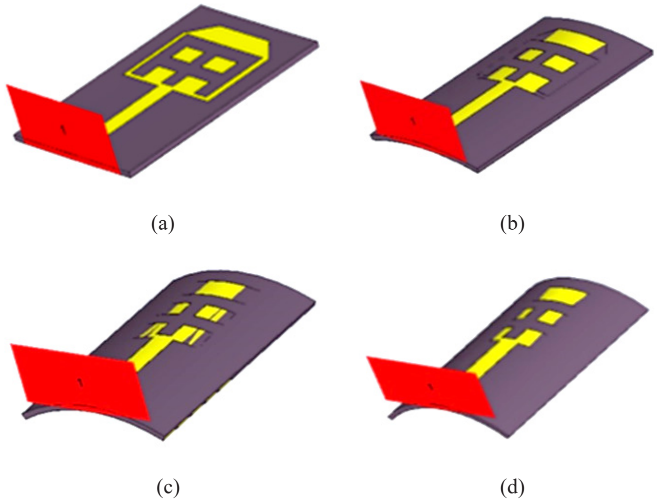

Fig. 9. Typical bent antenna image at 0⁰ angle (a), 30⁰ angle (b), 60⁰ angle (c), and 90⁰ angle (d).

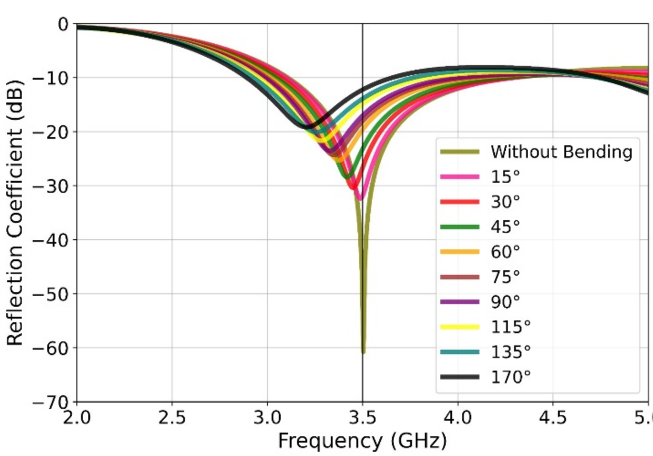

Fig. 10. S11 of the proposed antenna under various bending conditions.

Antenna performance metrics for each bending angle are summarized in Table II. It is observed that as the bending angle increases, radiation efficiency and gain decreases. When an antenna is bent, it typically broadens its radiation pattern in the bending plane, reducing the maximum radiation intensity in the desired direction, which lowers the overall gain [21]. Antenna efficiency decreases with increased bending because the deformation alters the antenna's physical structure, resulting in impedance mismatch, surface wave losses, and frequency shifting. These effects lead to a redistribution of electrical currents and a reduction in the power radiated compared to the power accepted [22]. The table also shows that antenna bandwidth decreases as bending increases. Bending the antenna changes its effective length and the electrical distance between the radiating patch and ground plane, thereby narrowing the frequency range for efficient operation [23].

TABLE II
BENDING ANALYSIS OF THE PROPOSED ANTENNA

Bending angle (degree)	Resonance frequency (GHz)	S11 at resonance (dB)	Bandwidth (GHz)	Radiation Efficiency (%)	Gain (dB)
0	3.50	-60.73	1.17	94.53	2.59
15	3.33	-32.39	1.21	93.36	2.59
30	3.44	-30.40	1.20	92.40	2.48
45	3.42	-28.43	1.19	91.65	2.56
60	3.38	-25.31	1.08	90.94	2.52
75	3.35	-24.32	1.05	90.33	2.49
90	3.33	-23.55	1.01	89.82	2.48
115	3.29	-21.68	0.89	89.05	2.41
135	3.26	-20.09	0.84	88.76	2.36
170	3.20	-19.17	0.76	87.01	2.26

C. Phantom Modeling and On-Body Results

1) 3D Phantom Modeling and Distance Optimization

The close integration of wearable antennas with the human body necessitates careful consideration of antenna–tissue interactions and their influence on key performance metrics. A human body phantom model was used with dimensions of $70 \times 60 \times 8$ mm^3. The phantom consisted of three layers: skin, fat, and muscle tissues with thicknesses of 2 mm, 3 mm, and 10 mm, respectively. Table III shows the electrical characteristics of the three tissue layers at a frequency of 3.5 GHz. The CST Studio Suite was used to create a body phantom model, as shown in Fig. 11(a). The electrical properties of skin, fat, and muscle tissues within the antenna's operating range were derived from the data reported in [24], [25] and are listed in Table III.

TABLE III
ELECTRICAL CHARACTERISTICS OF TISSUE LAYERS

Name of Tissue	Frequency (GHz)	Per-mi-ttivity (ϵ_r)	Con-duc-tivity σ (s/m)	Loss Tangent	Mass density (kg/m^3)
Skin (dry)	3.5	37.005	2.0249	0.28103	1109
Fat	3.5	5.1739	0.15553	0.15439	911
Muscle	3.5	51.444	2.5575	0.25533	1090

To determine the optimum distance, five different separation levels between the antenna and the human body phantom model were evaluated. As shown in Fig. 11(b), when the designed antenna was positioned very near the human body, the S11 values decrease, and the resonance peak shifts toward higher frequencies. This shift may be caused by fringing effects, which alter the effective width of the antenna structure when it comes near the human body. At a separation of 10 mm, the resonant peak was observed at 3.5 GHz. Based on these findings and considering the practical application of positioning the antenna over clothing such as a jacket or suit, rather than directly on the skin a 10 mm gap is identified as the optimal separation distance for this study.

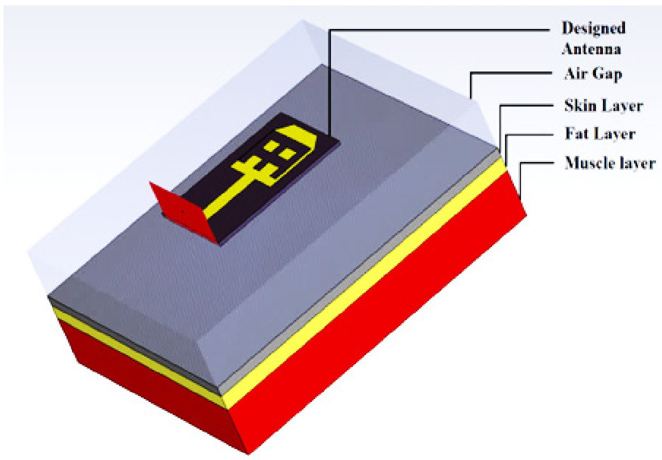

(a)

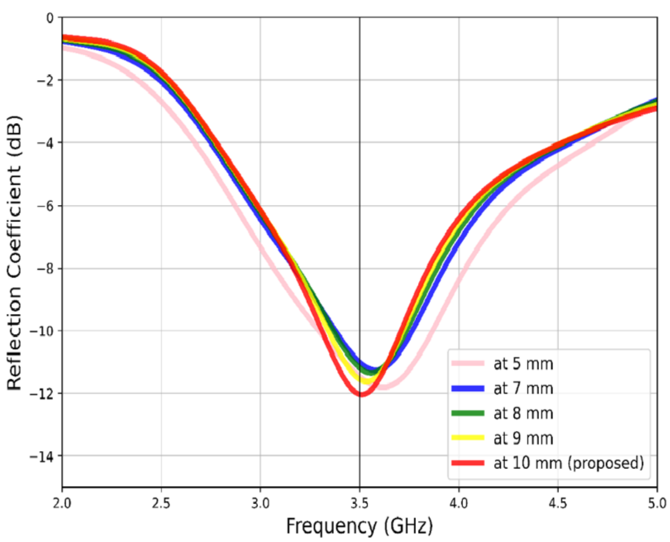

(b)

Fig. 11. On-body performance analysis of the antenna. (a) Three-layer tissue-equivalent phantom model. (b) Simulated S11 response.

2) On-body Simulation and Testing Results

Fig. 11(b) illustrates the reflection coefficient (S11) of the proposed antenna when placed on the human body phantom model with a 10 mm separation. The corresponding on-body performance metrics are presented in Table IV. At the resonant frequency of 3.5 GHz, the S11 value is -12.02 dB, which is lower than that observed under the off-body condition. Nonetheless, it remains well below the -10 dB threshold, indicating satisfactory impedance matching. The increased return loss can be attributed to reactive loading from the body and modifications to the antenna's input impedance caused by fringing effects. Under these on-body conditions, the antenna also sustains a wide bandwidth of 400 MHz. The VSWR at 3.5 GHz is measured at 1.66, further confirming adequate impedance matching.

At 3.5 GHz, the antenna achieves a gain of 2.14 dB, which is slightly lower than the 2.59 dB observed under off-body conditions. This reduction is likely due to electromagnetic energy absorption within the tissue layers of the phantom. A corresponding decrease in efficiency is also observed in the on-body case, consistent with these absorption effects. At 3.5 GHz, the radiation efficiency is measured at 34.06%, while the total efficiency is 36.34%.

TABLE IV
Performance Metrics of Proposed Antenna in On-Body Scenarios

Substrate Material	S11 (dB)	VSWR	Efficiency (%)		Bandwidth (MHz)	Gain (dB)
			Total	Radiation		
Polyester	-12.02	1.66	36.34	34.06	399.2	2.13

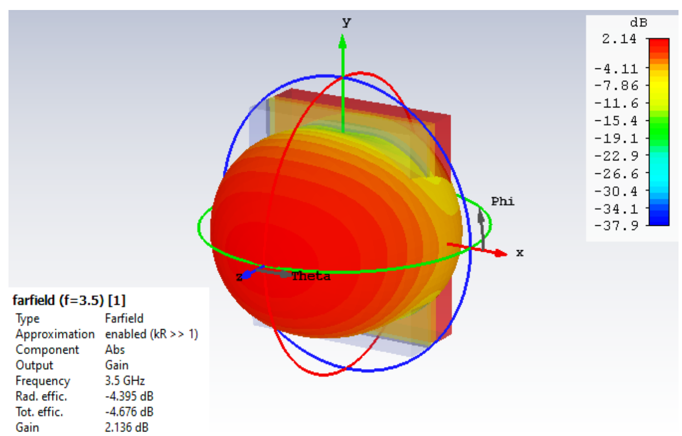

Fig. 12. Radiation pattern of the proposed antenna on phantom at 3.5 GHz.

The simulated 3D radiation pattern of the proposed antenna at 3.5 GHz over the human body phantom model is shown in Fig. 12. This result indicates that the antenna radiates moderately well at 3.5 GHz with a maximum gain of 2.136 dB and a radiation efficiency of -4.395 dB (~36%). The 3D plot shows the spatial distribution of the radiated power, which is mostly uniform but stronger in specific directions (as shown by the red/orange areas). The pattern is nearly spherical and omnidirectional, with the antenna radiating almost equally in many directions, with only slight preference in one direction (indicated by the small red lobe in the pattern). This pattern is suitable for Wi-Fi access points, IoT (Internet of Things) devices, and 5G / LTE small cells devices. Due to the low gain and near-spherical pattern, this antenna is also ideal for small form-factor wearable or embedded devices where consistent coverage in all directions is more important than long-range.

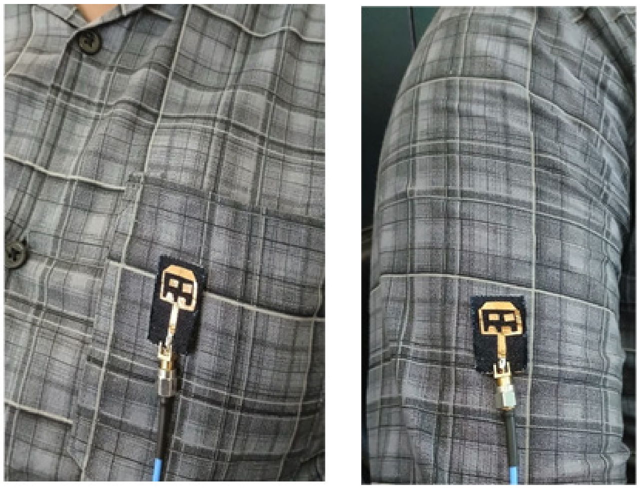

(a) (b)

Fig. 13. Placement of the proposed antenna to the (a) chest and (b) arm regions of the human body.

Fig. 13 illustrates the placement of the proposed antenna on the chest and arm regions of the human body for on-body measurements. The reflection coefficient responses obtained experimentally from various body locations are presented in Fig. 14. In free space, the fabricated antenna exhibited a resonant frequency of 3.54 GHz (Fig. 4). Upon placement on the arm, a downward shift in the resonance frequency to 3.4 GHz was observed, while the center frequency remained stable at 3.5 GHz when positioned on the chest. These results confirm that the proposed textile antenna effectively covers the entire frequency band required for broadband wireless applications.

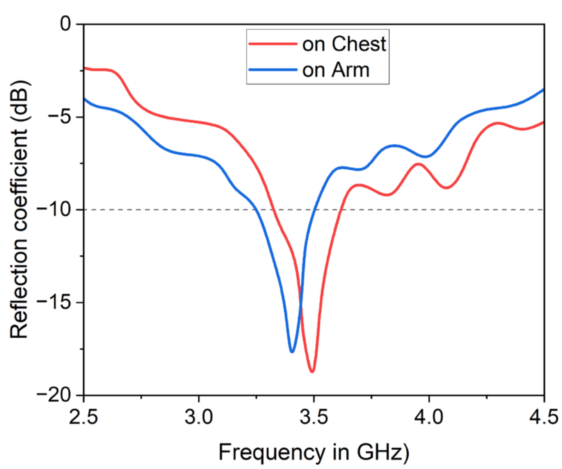

Fig. 14. Measure S11 on chest and arm regions of the human body.

D. SAR Analysis

The Specific Absorption Rate (SAR) quantifies the amount of electromagnetic (EM) energy absorbed per unit mass of human tissue. For wearable applications, it is essential to ensure that radiation from the designed antenna directed toward the human body remains within safe limits. According to regulatory standards, the maximum permissible SAR limit is 1.6 W/kg averaged over 1 gm of tissue, as defined by the U.S. Federal Communications Commission (FCC), and 2 W/kg averaged over 10 gm of tissue, as specified by the International Commission on Non-Ionizing Radiation Protection (ICNIRP).

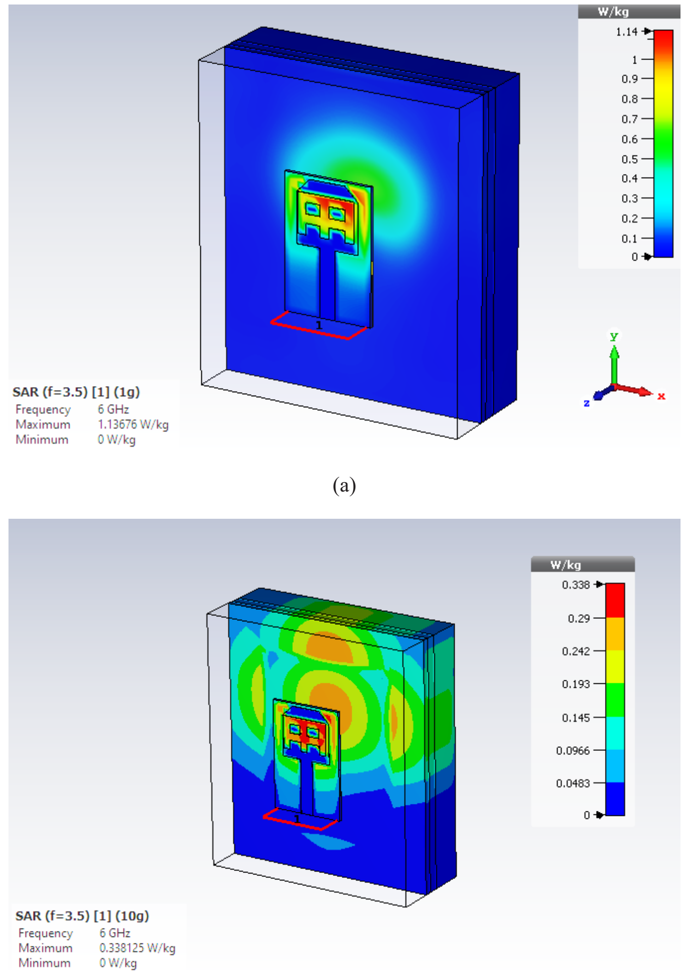

(b)

Fig. 15. SAR analysis over 1 gm (a) and 10 gm (b) of tissue for the body phantom model at 3.5 GHz.

In this work, SAR values were evaluated using a three-layer flat body phantom model, considering both 1 g and 10 g of tissue. An input power of 500 mW was applied in CST simulations to assess SAR performance at the operating frequency of 3.5 GHz. The resulting SAR values, shown in Fig. 15, are 1.137 W/kg for 1 g and 0.338 W/kg for 10 g of tissue. Both values are well below the safety thresholds established by the FCC, confirming the antenna's compliance with human exposure standards.

Although the typical power levels lie within 10-100mW in wearable devices, in the present SAR study a higher input power (500 mW) is used to simulate worst-case exposure conditions. It helps to ensure that even under extreme usage, the antenna remains within safety limits. It also ensures that even if the antenna operates above its intended power due to malfunction or environmental factors, it won't exceed SAR safety thresholds [26], [27].

V. Comparative Studies

A comparison of various performance metrics of the proposed antenna with other existing antennas published in earlier studies is provided in Table V. The present work with antenna size 30×20×0.8 mm³ achieves a compact footprint, smaller than most references, making it more suitable for integration into textiles. Polyester substrate is used in this work, which is flexible, durable, comfort and textile-compatible, unlike Paper or Kapton substrates used in some references. This work offers the largest bandwidth 1.17 GHz (covers 3.11 – 4.27 GHz), which is wider than reported values (≤0.6 GHz) in references [15], [28]-[31], ensuring multi-band operation. The antenna provides nearly 2.7 times wider bandwidth than average indicating robust against detuning from bending/stretching. This work achieves gain of 2.59 dB, which is nearly 1.8 dB higher than the average of references (~0.8 dB), ensuring stronger radiation performance and indicating stronger link margin for wearable communication. With 94.52% efficiency, this work is among the highest reported, only slightly below the reference [31] (99.5%), but significantly better than most others.

The radiation efficiency is nearly 11% higher than average indicating reliable radiation in textile environments. This work shows SAR values of 1.134 W/kg (1g) and 0.338 W/kg (10g), which are within IEEE/FCC safety limits (<1.6 W/kg for 1g) for body-worn devices, and comparable to other wearable designs. It balances safety with performance, indicating suitable for body-worn applications. This Work achieves the best balance of bandwidth, efficiency, and robustness, making it ideal for smart clothing applications where flexibility, safety, and reliable performance are essential.

Hence the present polyester flexible patch antenna is more robust than the references because it combines wider bandwidth, higher efficiency, moderate gain, and stable performance under bending, while maintaining safe SAR levels and a compact textile-compatible design. This robustness directly translates into superior suitability for smart clothing applications, where antennas must remain reliable under bending, stretching, and daily wear conditions.

TABLE V
Performance Comparison of the Proposed Antenna with the Previous Work at 3.5 GHz Band

Design Parameter	**Reference No.**						
	[15]	**[16]**	**[28]**	**[29]**	**[30]**	**[31]**	**This Work**
Antenna Size (mm^3)	30× 30× 1.6	40× 40× 0.44	70× 70× 2.1	40× 77× 0.6	60× 60× 1.17	27.4× 15.6× 0.125	30× 20× 0.8
Substrate/ Permittivity	Jeans/ Denim/ 1.7/ 1.67	Photo Paper/ 3.2	Felt/ 1.634	Denim/ 1.78	Denim/ 1.78	Kapton HN/ 3.4	Polyester/ 1.9
Operating Range (GHz)	3.15 – 3.95	3.33– 3.75	3.46– 3.76	~3.4 – 4.0	2.2 –4.0	3.26– 3.80	3.11 – 4.27
Bandwidth (GHz)	0.540	—	0.3	0.6	0.19	0.545	1.17
Gain (dB)	—	1.4	0.3	3	−2.81	2.07	2.59
Efficiency (%)	—	70	—	~80	—	99.5	94.52
SAR (W/Kg)	—	—	0.57 (1g)	1.03 (1g)/ 0.92 (10g)	0.11 (1g)/ 0.33 (10g)	—	1.134 (1g) 0.338 (10g)

VI. Conclusion

In this work, a compact polyester substrate-based textile microstrip patch antenna operating in the 3.5 GHz band has been successfully designed, fabricated, and validated for next-generation wearable broadband applications. By addressing all critical aspects—including off-body performance, fabrication, testing, on-body evaluation, bending analysis, and SAR assessment—the study provides a comprehensive framework that has been largely absent in prior research. The proposed antenna demonstrates wide bandwidth, high radiation efficiency, and stable performance under bending conditions, while maintaining compliance with IEEE SAR safety standards. Covering multiple bands such as 5G NR (n77, n78), C-Band, CBRS, and extended C-Bands, the antenna proves to be robust, cost-effective, and well-suited for integration into smart clothing. Overall, this work establishes polyester textile antennas as a promising solution for wearable wireless systems, combining practicality, safety, and reliable performance in real-world scenarios.

In experimental work, a single antenna sample was fabricated and experimentally tested. The presented results are based on one measurement, which provides an initial validation of the design concept. While these findings demonstrate the feasibility and performance of the proposed antenna, a statistical analysis across multiple fabricated samples and repeated measurements has not yet been conducted. Future studies will focus on fabricating additional prototypes and performing repeated measurements to assess reproducibility, quantify measurement uncertainty, and establish statistical reliability in the reported performance. Additionally, the antenna's gain, efficiency, and radiation pattern will be measured in an anechoic chamber to provide further experimental validation. Long-term durability tests—such as repeated bending and washing cycles under sustained mechanical stress—will also be conducted to reinforce the claims of suitability for smart clothing applications.

References

[1] S. K. Koul, R. Bharadwaj, "Introduction to Body Centric Wireless Communication," *Wearable Antennas and Body Centric Communication*," Lecture Notes in Electrical Engineering, vol 787, Springer, Singapore, 2021, DOI: 10.1007/978-981-16-3973-9_1.

[2] A. Alemaryeen and S. Noghanian, "On-Body Low-Profile Textile Antenna with Artificial Magnetic Conductor," *IEEE Transactions on Antennas and*

Propagation, vol. 67, no. 6, pp. 3649-3656, June 2019, DOI: 10.1109/TAP.2019.2902632.

[3] R. K. Singh, A. Michel, P. Nepa, A. Salvatore, M. Terraroli and P. Perego, “Compact and Wearable Yagi-Like Textile Antennas for Near-Field UHF-RFID Readers,” *IEEE Transactions on Antennas and Propagation*, vol. 69, no. 3, pp. 1324-1333, March 2021, DOI: 10.1109/TAP.2020.3030944.

[4] N.I. Zaidi, N.H.A. Rahman, M.F. Yahya, M.S.A. Nordin, S. Subahir, Y. Yamada, A. Majumdar, “Analysis on Bending Performance of the Electro-Textile Antennas with Bandwidth Enhancement for Wearable Tracking Application,” *IEEE Access*, vol. 10, pp. 31800-31820, 2022, DOI: 10.1109/ACCESS.2022.3160825.

[5] F.F. Hashim, W.N.L.B. Mahadi, T.B.A. Latef, M. Bin Othman, “Key Factors in the Implementation of Wearable Antennas for WBNs and ISM Applications: A Review WBNs and ISM Applications: A Review,” *Electronics*, vol. 11, no. 15, pp. 2470, August 2022, DOI: 10.3390/electronics11152470.

[6] E. Çelenk and N.T. Tokan, “All-Textile On-Body Antenna for Military Applications,” *IEEE Antennas and Wireless Propagation Letters*, vol. 21, no. 5, pp. 1065-1069, May 2022, DOI: 10.1109/LAWP.2022.3159301.

[7] C.G. Bartone, L. Moore, M. Kohli, “An e-textile antenna for body area network,” *Proceedings of the 2016 IEEE International Symposium on Antennas and Propagation (APSURSI)*, Fajardo, PR, USA, 26 June 2016–1 July 2016; pp. 999–1000, DOI: 10.1109/APS.2016.7696208.

[8] S. Khan, V. K. Singh, B. Naresh, “Textile antenna using jeans substrate for wireless communication application,” *Int. J. Eng. Tech. Sci. Res.,* 2015, 2, 176–181, [Online] Available: www.ijestr.com

[9] A.W. Memon, I.L. Depaula, B. Malengier, S. Vasile, P. Van Torre, L. Van Langenhove, “Breathable Textile Rectangular Ring Microstrip Patch Antenna at 2.45 GHz for Wearable Applications,” *Sensors*, vol. 21, no. 5, pp. 1635, 2021, DOI: 10.3390/s21051635.

[10] G. Mollah, K. Shikder and F. Arifin, “Design and Evaluation of a SWB Decagonal Patch Textile Antenna for WBAN Applications,” *IEEE Region 10 Symposium (TENSYMP)*, Dhaka, Bangladesh, 2020, pp. 1420-1423, DOI: 10.1109/TENSYMP50017.2020.9230812.

[11] D.-G.Kang, J. Tak, J. Choi, “MIMO Antenna with High Isolation for WBAN Applications,” *Int. J. Antennas Propag.*, vol. 2015, Article ID: 370763, pp. 1-7, 2015, DOI: 10.1155/2015/370763.

[12] K. Ali, S. Ali, H. R. Chowdhury, A. Ahmed, “Design and performance analysis of a textile antenna suitable for smart clothing,” *IEEE Region 10 Humanitarian Technology Conference (R10-HTC)*, Dhaka, Bangladesh, 2017, pp. 367-370, DOI: 10.1109/R10-HTC.2017.8288976.

[13] L. Zhou, S. Fang and X. Jia, “Dual-band and dual-polarised circular patch textile antenna for on-/off-body WBAN applications,” *IET Microwaves*, Antennas & Propagation Volume 14, Issue 7, February 2020, DOI: 10.1049/iet-map.2019.1073.

F.A Tahir, A. Javed, “A compact dual-band frequency reconfigurable textile antenna for wearable applications,” *Microw Opt Technol Lett.*, vol. 57, no. 10, pp. 2251–2257, 2015; DOI:10.1002/mop.29311.

[14] V. Kavitha, K. Malaisamy, T.S. Murugesh and M. S. Kumar, “Design and development of jeans textile antenna for wireless broadband applications,” *Journal of Industrial Textile*, Vol. 53, pp. 1–13, December 6, 2023, DOI: 10.1177/15280837231215374.

[15] A.K. Singh, S. K. Mahto, R. Sinha, M. Alibakhshikenari, A. J. A. Al-Gburi, A. Ahmad, L. Kouhalvandi, B.S. Virdee, and M. Dalarsson, “Low-Loss Paper-Substrate Triple-Band-Frequency Reconfigurable Microstrip Antenna for Sub-7 GHz Applications,” *Sensors*, 23, 8996, November 2023, DOI:10.3390/s23218996.

[16] M. M. Hasan, and A.Z.M.T. Islam, “A Wideband Compact Flexible Patch Antenna Design on Polydimethylsiloxane (PDMS) for Wearable Technology,” *Cureus J Eng*, Vol. 2, es44388-025-04462-7, April 2025, DOI:10.7759/s44388-025-04462-7.

[17] D. Ferreira, P. Pires, R. Rodrigues, and R. F. S. Caldeirinha, “Wearable textile antennas: examining the effect of bending on their performance,” *IEEE Antennas and Propagation Magazine*, vol. 59, no. 3, pp. 54–59, 2017, DOI: 10.1109/MAP.2017.2686093.

[18] A. Mersani, L. Osman, and J. M. Ribero, “Effect of bending on the characteristics of a Coplanar Textile Antenna,” *Proc. of 18th Mediterranean Microwave Symposium MMS*, pp. 255-257, 2018, DOI: 10.1109/MMS.2018.8612049.

[19] S. M. Salleh, M. F. Ain, Z. Ahmad, I.S.Z. Abadin, and C.M.N.C. Isa, “Development of Stretchable and bendable polymer wearable antenna for 5G Applications,” *Express Polymer Letters*, Vol. 16, No. 12, pp. 1267-1279, Nov. 12, 2022, DOI: 10.3144/expresspolymlett.2022.92.

[20] Y. Mukai, V.T. Bharambe, J.J. Adams, and M. Suh, “Effect of bending and padding on the electromagnetic performance of a laser-cut fabric patch antenna,” *Textile Research Journal*, 2019;89(14):2789-2801, DOI: 10.1177/004051751880120.

[21] P. Salonen, M. Keskilammi and Y. Rahmat-Samii, “Textile antennas: Effect of antenna bending on radiation pattern and efficiency,” *IEEE Antennas and Propagation Society International Symposium*, San Diego, CA, USA, 2008, pp. 1-4, DOI: 10.1109/APS.2008.4619343.

[22] N. A. Elias, N. A. Samsuri, M. K. A. Rahim, C. Panagamuwa, and W. Whittow, “Bending and crumpling deformation study of the resonant characteristic and SAR for a 2.4 GHz textile antenna,” *J. Teknol.*, vol. 177, no. 10, 2015, DOI: 10.11113/jt.v77.6278.

[23] P. A. Hasgall, F. Di Gennaro, C. Baumgartner, E. Neufeld, B. Lloyd, M. C. Gosselin, D. Payne, A. Klingenböck, and N. Kuster, *IT'IS Database for thermal and electromagnetic parameters of biological tissues*, Version 4.1, Feb. 22, 2022, DOI: 10.13099/VIP21000-05-0.

[24] D. Andreuccetti, R.Fossi and C.Petrucci, “An Internet resource for the calculation of the dielectric properties of body tissues in the frequency range 10 Hz - 100 GHz,” *IFAC-CNR*, Florence (Italy), 1997. Based on data published by C.Gabriel et al. in 1996. [Online]. Available: http://niremf.ifac.cnr.it/tissprop/.

[25] J. C. Wang, E. G. Lim, M. Leach, Z. Wang and K. L. Man, “Review of SAR Measurement Methods in Relation to Wearable Devices,” *Engineering Letters*, vol. 24, no. 3, 2016, DOI: 10.1063/5.0206045.

[26] P. Zradziński, J. Karpowicz, K. Gryz, “The Parametrization of Electromagnetic Emissions and Hazards from a Wearable Device for Wireless Information Transfer with a 2.45 GHz ISM Band Antenna,” *Appl. Sci.*, vol. 15, no. 12, 2025, 6602, DOI: 10.3390/app15126602.

[27] S. Bhattacharjee and M. Mitra, “Triple Band Compact Textile Antenna Structure for Wearable Applications,” *Progress In Electromagnetics Research C*, Vol. 144, 1-8, 2024, DOI:10.2528/PIERC24031306.

[28] M. A. Abdelghany, M. I. Ahmed, A. A. Ibrahim, A. Desai and M. F. Ahmed, “Textile Antenna with Dual Bands and SAR Measurements for Wearable Communication,” *Electronics*, 13 (12), 2251, 2024, DOI: 10.3390/electronics13122251.

[29] H. Li, J. Du, X. -X. Yang and S. Gao, “Low-Profile All-Textile Multiband Microstrip Circular Patch Antenna for WBAN Applications,” *IEEE Antennas and Wireless Propagation Letters*, vol. 21, no. 4, pp. 779-783, April 2022, DOI: 10.1109/LAWP.2022.3146435.

[30] Z. Hossain, A. K. M., N. B. Hassim, S. M. K. Azam, M. S. Islam, and M. K. Hasan, “A planar antenna on flexible substrate for future 5G energy harvesting in Malaysia,” *International Journal of Advanced Computer Science and Applications (IJACSA)*, Vol. 11, No. 10, 2020, DOI: 10.14569/IJACSA.2020.0111020.